EUROPEAN ORGANIZATION FOR NUCLEAR RESEARCH

Ref. TH.1290
22 February 1971.

THEORY AND PRACTICE OF COMPLEX REGGE POLES

F. Zachariasen*)

CERN, Geneva, Switzerland.

Lectures given at the
X Internationale Universitätswochen Kernphysik,
Schladming 28 February - 13 March 1971.

*) J.S. Guggenheim Memorial Foundation Fellow, on leave from Calif. Inst. of Technology, Pasadena, Calif., USA.

1. INTRODUCTION

In the form in which it was originally put forward, Regge phenomenology contained a wealth of predictions. If Regge poles alone dominated scattering amplitudes at high energies, then the simple form taken by a single Regge pole term, together with factorization of Regge residues, permitted one to parametrize scattering amplitudes with only very few unknowns, and also dictated very specific relations between scattering amplitudes describing different processes.

As it has turned out, however, this admirable vision of high-energy phenomenology has failed. It is simply not true that in general Regge poles alone dominate; other kinds of j-plane singularities, specifically branch points, are also present and are important.

If cuts, as well as poles, are necessary to parametrize high-energy amplitudes, what is left of the predictive power of Regge theory? In the absence of any knowledge about the cuts, one would at first expect almost nothing. The fact that an unknown j-plane cut has an arbitrary function of two variables (t and j) as its discontinuity means that one can fit essentially any scattering amplitude (which is, after all, also only a function of two variables) with a cut. Furthermore, because factorization fails in the presence of cuts, no predictions remain which relate different scattering processes to each other. Essentially the only prediction which obviously remains is that scattering amplitudes, at a given value of t, behave like powers of s at large s (apart from logarithmic factors).

Therefore, if Regge theory is not to be discarded as basically vacuous, it is necessary to discover some theoretical limitations on the cuts. What then do we know about j-plane cuts?

That cuts should, theoretically, be expected to exist was first shown by Mandelstam[1,2]. He found, by studying a particular class of Feynman graphs, that if two Regge poles with trajectories $\alpha_1(t)$ and $\alpha_2(t)$ existed, then one also had a cut with a branch point at $\alpha_c(t) = \alpha_1(t/4) + \alpha_2(t/4) - 1$. In particular, if one of the two poles (say α_2) were the Pomeranchon (assuming that it indeed exists) with $\alpha_P(0) = 1$, we find $\alpha_c(0) = \alpha_1(0)$, and the cut and pole α_1 have the same quantum numbers; that is, they occur in the same amplitude. In addition, since the slope of the branch point

is less than the slope of the pole $\alpha_1(t)$, it lies above the pole for $t < 0$ but below for $t > 0$.

This branch point, formed by the interference of two poles, may well exist. But is it the highest branch point? For example, if a pole $\alpha_1(t)$ and the Pomeranchon $\alpha_P(t)$ generate a cut with branch point at $\alpha_c(t) = \alpha_1(t/4) + \alpha_P(t/4) - 1$, then the cut itself together with another Pomeranchon should, by the same argument, be expected to generate another cut with branch point at $\alpha_c^{(2)}(t) = \alpha_c(t/4) + \alpha_P(t/4) - 1$; this second cut has even smaller slope than the first one, yet still satisfies $\alpha_c^{(2)}(0) = \alpha_1(0)$, so it lies above the first cut for $t < 0$.

Such arguments may be repeated, making plausible the existence of a sequence of branch points with smaller and smaller slopes, all crossing the original trajectory $\alpha_1(t)$ at $t = 0$.

To summarize, then, we can say only the following about the position of branch points in the j-plane: given a pole $\alpha_1(t)$, there exists a branch point $\alpha_c(t)$ with the same quantum numbers such that $\alpha_c(0) = \alpha_1(0)$, and which lies above $\alpha_1(t)$ for $t < 0$. Even this feeble conclusion, we should note, depends on the existence of a Pomeranchon with $\alpha_P(0) = 1$; if $\alpha_P(0)$ is slightly less than one (as some models suggest) then the pole and cut cross at some finite negative value of t. The various cases are illustrated in Fig. 1.

Can there be other cuts as well as these? Of course there can. Specific models yielding different cuts exist. For example, one such model gives a flat cut associated with each pole $\alpha_1(t)$ crossing the pole at $t = 0$: $\alpha_c(t) = \alpha_1(0)$ [3]. The only thing we can do is, optimistically, to believe that the only cuts which exist are those for which we can find specific theoretical arguments.

The most important characteristic of a cut, which we would like to know if we are to be able to make any experimental predictions, is the nature of the branch point. The first Mandelstam cut, generated by two Regge poles, turns out to be logarithmic[1,2]; that is, the t-channel partial wave amplitude has the form $T(t,j) \sim \log (j - \alpha_c(t))$. Successive cuts, however, have more complicated types of singularities[2]. Other models[3] lead to cuts with square root singularities: $T(t,j) \sim \sqrt{j - \alpha_c(t)}$.

Obviously, we can say nothing which is model independent.

The same is true about the third characteristic of cuts which we would like to know; that is the actual value of the discontinuity across the cut. Any statement we can make is model dependent: the discontinuity of the first Mandelstam cut can be calculated in terms of the poles (and their residues) which generate it. The same is the case for the cut in other specific models; however the answers in the various models are all different.

To summarize, perhaps the only thing which we can safely say on (nearly) model independent grounds is that there exists a cut associated with each Regge pole, occuring in the same amplitude, which is flatter than the pole and which crosses it at or near $t = 0$. All other details, such as the type of branch point or the value of the discontinuity, are model dependent.

If we wish not to commit ourselves to specific [and doubtless wrong[4)]] models, is there then anything left to say? Can we make any phenomenological predictions at all? The answer is yes, as we shall see below. What we shall do is to accept from the foregoing discussion only the (probably) reliable statement about the position of the branch point. Then, using only this input, we shall on the basis of general (and incontrovertible) principles such as unitarity argue that it may still be possible to make certain non-trivial phenomenological predictions. These predictions will, of course, be less detailed than those which could be made on the basis of specific models; but they will, in contrast, have a chance of being right.

2. THE FORM OF THE t-CHANNEL PARTIAL WAVE AMPLITUDE

The crucial principle which we must maintain is t-channel unitarity. (This, incidentally, is entirely ignored in the specific cut models now commonly in use).

We assume that the t-channel partial wave amplitude[5] $T(t,j)$ has a branch point at $j = \alpha_c(t)$. Because $T(t,j)$ must satisfy unitarity, it is reasonable to suppose that the corresponding D function $D(t,j)$ also contains a branch point at $j = \alpha_c(t)$. In the neighbourhood of the branch point, we may write the contribution of the branch point in D explicitly; the remainder of D is then smooth in j and, near $j = \alpha_c$, we may expand it in powers of j. Then we may write, near $j = \alpha_c$,

$$D(t,j) = j - \alpha_c(t) - D_c(t,j) \tag{2.1}$$

where $D_c(t,j)$ contains the cut. (This may be thought of as a sort of effective range expansion in j. Since the normalization of D is arbitrary, we choose the coefficient of j equal to one.)

Let us, by means of some examples and other arguments, understand why this form is to be expected, and make clear what is meant by the function D_c[6].

First, suppose we start with a model for the partial wave amplitude containing a pole at $\alpha_{in}(t) = \alpha_0 + \alpha_1 t$ (α_0 and α_1 are real), and a cut, added to each other. (As, for example, in the absorption model.) We write as the input partial wave amplitude

$$T_{in}(t,j) = \frac{\beta_{in}(t)}{j - \alpha_{in}(t)} + T_c(t,j) \tag{2.2}$$

where $T_c(t,j)$ is the (explicit) cut term in the model. This amplitude is manifestly not unitary. Suppose we unitarize it, by, say the K-matrix method. Then we write the unitarized amplitude as

$$T(t,j) = \frac{T_{in}(t,j)}{1 - i\rho(t)\,T_{in}(t,j)} \tag{2.3}$$

where $\rho(t)$ is a phase space factor. (Note that ρ is real for t above threshold, and imaginary for t below threshold.) Then we find

$$T(t,j) = \frac{\beta_{in} + (j - \alpha_{in}) T_c}{j - \alpha_{in} - i\rho(\beta_{in} + (j - \alpha_{in}) T_c)} \tag{2.4}$$

so that

$$D(t,j) = j - \alpha_0(t) - D_c(t,j) \tag{2.5}$$

where

$$\alpha_0(t) = \alpha_{in}(t) + i\rho(t)\beta_{in}(t)$$

and where

$$D_c(t,j) = i\rho(t)(j - \alpha_0(t)) T_c(t,j) \,. \tag{2.6}$$

If the cut is absent ($T_c = 0$), then the resulting trajectory in the unitarized amplitude is simply $\alpha_0 = \alpha_{in} + i\rho\beta_{in}$; i.e. Im $\alpha_0(t) = \rho(t)\beta_{in}(t)$ for t above threshold, a well known result.

Thus one may think of $\alpha_0(t)$ as a sort of unperturbed trajectory, which is altered (thorugh unitarity) by the cut into a new trajectory $\alpha(t)$. The new trajectory, of course, is the solution to

$$D(t, \alpha(t)) = 0 \tag{2.7}$$

Secondly, suppose we unitarize the amplitude of Eq. (2.2) by a slightly more sophisticated method, say the N over D method. We choose N to be[7]

$$N(t,j) = \beta_{in}(t) + (j - \alpha_{in}(t)) T_c(t,j) \,. \tag{2.8}$$

Then it follows that D is given by

$$D(t,j) = j - \alpha_{in} - \frac{1}{\pi}\int_{t_c}^{\infty} \frac{\rho(t')\,dt'}{t'-t}\left(\beta_{in}(t') + (j-\alpha_{in}(t'))\,T_c(t',j)\right) \tag{2.9}$$

so that we now identify

$$\alpha_0(t) = \alpha_{in}(t) + \frac{1}{\pi}\int_{t_c}^{\infty} \frac{\rho(t')\,dt'}{t'-t}\,\beta_{in}(t') \tag{2.10}$$

and

$$D_c(t,j) = \frac{1}{\pi}\int_{t_c}^{\infty} \frac{\rho(t')\,dt'}{t'-t}\left((j-\alpha_{in}(t'))\,T_c(t',j)\right) . \tag{2.11}$$

The same interpretation as before is natural.

As a third illustration, and confirmation, of the form (2.1) let us revert to potential theory. Recall the situation when two Regge poles $\alpha_0(t)$ and $\alpha_1(t)$, cross[8]. The D function is a quadratic form in j near the collision point, and may be written as

$$D(t,j) = \det \begin{vmatrix} j-\alpha_0(t) & \epsilon_1(t) \\ \epsilon_1(t) & j-\alpha_1(t) \end{vmatrix} . \tag{2.12}$$

Evidently solutions of $D(t,\alpha) = 0$ are either two real poles or a complex conjugate pair. Thus when two poles collide, they become a complex conjugate pair of poles[8]. One may interpret ϵ_1 as the"coupling" of the two poles, and one may say that an unperturbed trajectory α_1 is perturbed by the presence of another trajectory α_1 into a new trajectory α which is the solution of $D(t,\alpha) = 0$.

Next suppose the unperturbed pole α_0 collides with a family of other poles α_i, $i = 1 \ldots \infty$ [9]

In analogy with Eq. (2.12), we write

$$D(t,j) = \det \begin{vmatrix} j-\alpha_0 & \epsilon_1 & \epsilon_2 & \cdots \\ \epsilon_1 & j-\alpha_1 & 0 & \\ \epsilon_2 & 0 & j-\alpha_2 & \\ \vdots & & & \end{vmatrix}$$

$$= \left(j - \alpha_0 - \sum_{i=1}^{\infty} \frac{\epsilon_i^2}{j-\alpha_i}\right) \exp \sum_{i=1}^{\infty} \log(j-\alpha_i) \qquad (2.13)$$

(We have here, for simplicity, neglecting "coupling" between the "other" trajectories α_i.) Now let the family of poles α_i all be parallel: we write $\alpha_i(t) = \alpha_1(t) - \delta(i-1)$. Then we let δ, the spacing, approach zero and call $\alpha_1(t) = \alpha_c(t)$. We have thus constructed the situation of an unperturbed pole α_0 perturbed by the presence of a continuum of parallel other poles; that is, by a cut. The D function [dropping the irrelevant exponential in Eq. (2.13)] is[9]

$$D(t,j) = j - \alpha_0(t) - \int_{-\infty}^{\alpha_c} \frac{\epsilon^2(t,j')}{j-j'}\, dj' \qquad (2.14)$$

Again, we recover the basic form (2.1).

As a final confirmation of Eq. (2.1), we may merely note that in two explicit dynamical models containing both poles and cuts this form appears. In all versions of the multiperipheral, or multi Regge, model, one finds[10] (at least approximately)

$$D(t,j) = j - \alpha_0(t) - \beta_0(t) \log(j - \alpha_c(t)) \qquad (2.15)$$

while in the Carlitz-Kislinger model[3] one finds

$$D(t,j) = j - \alpha_0(t) - \beta_0(t)\sqrt{j-\alpha_c(t)} \,. \qquad (2.16)$$

We take it then that the form (2.1) for the D function near $j = \alpha_c$ may be believed on a model independent basis. As we have seen, the way to interpret Eq. (2.1) is to think of an unperturbed Regge pole $\alpha_0(t)$ colliding with the cut contained in $D_c(t,j)$, and thus becoming altered into a new pole $\alpha(t)$, satisfying $D(t,\alpha(t)) = 0$. This interpretation is then entirely analogous to that of Eq. (2.12), where one

thinks of the original pole α_0 colliding with the pole α_1, and becoming altered to a new pole α. The only feature of the cut which we need to know in order to make this interpretation is the position of the branch point: this allows us to say that $\alpha_0(t)$ and $\alpha_c(t)$ "collide" at, or near, $t = 0$.

What do we learn from this about the behaviour of the output poles, the solutions to $D(t,\alpha) = 0$? Let us take the two specific models, Eqs. (2.15) and (2.16) as illustrations.

In the logarithmic cut example, there is one pole on the physical sheet, satisfying the equation

$$\alpha = \alpha_0 + \beta_0 \log(\alpha - \alpha_c)$$

We presume that α_0 and α_c cross at $t = 0$. Since the logarithm blows up as $\alpha \to \alpha_c$, the pole can never pass through the cut, but must instead approach it asymptotically. The situation is illustrated in Fig. 2.

There are also poles on all unphysical sheets, satisfying

$$\alpha_n = \alpha_0 + \beta_0 (\log(\alpha_n - \alpha_c) + i n \pi)$$

for $n = \pm 1, \pm 2 \ldots$. Evidently these occur in complex conjugate pairs, $\alpha_n = \alpha^*_{-n}$, and their imaginary part never vanishes. These complex poles can pass the cut, as sketched in Fig. 2.

A further comment of interest is the following[10]. The residue of the physical sheet pole is proportional to $(\partial D/\partial j)^{-1}|_{j=\alpha}$; that is, to $(\alpha - \alpha_c/\alpha - \alpha_c - \beta_0)$. Thus as $\alpha \to \alpha_c$, the residue becomes very small.

Hence the physical sheet pole becomes weak, and therefore unimportant, as t becomes more and more negative. This same situation does not obtain for the unphysical sheet poles. There, since $\mathrm{Im}\,\alpha \neq 0$ $\alpha - \alpha_c$ does not become small, so these poles are not, in general, weakly coupled. Thus, crudely speaking, the partial wave amplitude at negative t may be described as containing the cut and a (on the nearest unphysical sheets) complex conjugate pair of poles, moving through the cut, plus a weakly coupled (on the physical sheet) pole just above the cut. Poles on further unphysical sheets ($n \neq \pm 1, 0$) are, presumably, too far away to be of much interest.

The square root example is also easily analyzed[9]. There are now two sheets, and two poles α_+ and α_-, given by

$$\alpha_\pm = \alpha_0 + \beta_c^2/2 \pm \sqrt{\beta_c^4/4 + \beta_c^2(\alpha_0 - \alpha_c)}$$

Again we assume α_0 and α_c cross at $t = 0$. Poles with Re $\sqrt{\alpha} > 0$ are on the physical sheet, and poles with Re $\sqrt{\alpha} < 0$ are on the unphysical sheet.

As $t \to +\infty$, $\alpha_\pm$ approach α_0, the unperturbed pole, and α_+ lies on the physical sheet, while α_- is on the unphysical sheet. As t decreases, α_+ and α_- decrease too. At a negative (or zero if β_0 vanishes at $t = 0$) value of t, the two poles collide at a negative (or zero) value of $j - \alpha_c$. They are by this time both on the same sheet, α_+ having passed through the cut onto the unphysical sheet, or α_- having passed through the cut onto the physical sheet, depending on the sign of β_0. Below the point of collision, the two poles are a complex conjugate pair. This situation is illustrated in Fig. 3.

Thus the partial wave amplitude contains, at negative t, the cut and a complex conjugate pair of poles (on either the unphysical or physical sheet).

The effective situation is therefore very similar to the logarithmic case, and indeed one can convince oneself that the same is true for any type of cut: the partial wave amplitude will consist of a cut, plus complex conjugate pairs of poles on various sheets, plus (possibly) real poles.

3. THE FORM OF THE SCATTERING AMPLITUDE AT HIGH ENERGY[11)]

We learned in Section 2 what we may expect, independently of any model, for the t-channel partial wave amplitude; namely it contains a cut, complex pairs of poles, and (perhaps) real poles. Let us for simplicity suppose it to contain a cut and a single complex pair. (If there are in reality several complex pairs, the one we shall select is that with smallest imaginary part. If there are real poles, they will appear in the usual way). Thus we assume that T(t,j) has a branch point at $j = \alpha_c(t)$, and poles at $j = \alpha_\pm(t) = \alpha_R(t) \pm i\,\alpha_I(t)$.

Let us exhibit the poles explicitly, by writing

$$T(t,j) = \frac{f(t,j)}{(j-\alpha_+(t))(j-\alpha_-(t))} \quad . \tag{3.1}$$

The function f contains the cut, and the poles are on an unphysical sheet if $f(t,\alpha_\pm(t)) = 0$.

The high-energy scattering amplitude is constructed in the usual way by means of a Mellin transform:

$$T(s,t) = \frac{1}{2\pi i}\int_{C-i\infty}^{C+i\infty} \frac{s^j f(t,j)}{(j-\alpha_+)(j-\alpha_-)}\,dj \tag{3.2}$$

where C is larger than any singularity in T(t,j). We can now deform the contour in Eq. (3.2) to obtain

$$T(s,t) = \bar\beta_+ s^{\alpha_+} + \bar\beta_- s^{\alpha_-} + \frac{1}{\pi}\int_{-\infty}^{\alpha_c} \frac{s^j \operatorname{Im} f(t,j)}{(j-\alpha_+)(j-\alpha_-)}\,dj \tag{3.3}$$

where 2i Im f(t,j) is the discontinuity across the cut in f(t,j), and where

$$\bar\beta_\pm = \pm f(t,\alpha_\pm)/(\alpha_+ - \alpha_-) \quad . \tag{3.4}$$

Hence $\bar{\beta}_{\pm} = 0$ if the poles are on an unphysical sheet; and in general $\bar{\beta}_{+} = (\bar{\beta}_{-})^{*}$.

It is worth pointing out explicitly certain qualitative features of Eq. (3.3), and most particularly of the integral therein. This integral, evidently, exhibits the cut contribution to T(s,t). The weight function for the cut -- that is, the discontinuity across the cut -- is Im $f/[(j - \alpha_R)^2 + \alpha_I^2]$. If α_I is small, therefore, the weight function has a large Breit-Wigner like peak at $j = \alpha_R$. This tends to emphasize the $j = \alpha_R$ region of the integral, and suggests that the energy dependence ought to be approximately s^{α_R}, unless s is very large. If s is very large, however, then clearly the dominant behaviour will be s^{α_c}. How large is large, clearly, depends on the size of α_I, as well as on the form of Im f.

The size of α_I is, of course, proportional to the strength of the cut, as we have seen in Section 2; that is, α_I must be proportional to Im f. Therefore, as the cut becomes very weak, and vanishes, the integral in Eq. (3.3) approaches

$$\left(\frac{\partial \, \mathrm{Im} \, f(t, \alpha_R)}{\partial \alpha_I} \right)_{\alpha_I = 0} s^{\alpha_R} ,$$

and we recover the original single real pole with $\alpha_R = \alpha_0$, which we would have had if there were no cut at all.

For very weak cuts -- i.e. for very small α_I, we may conveniently rewrite Eq. (3.3) in the form

$$T(s,t) = \bar{\beta}_{+} s^{\alpha_+} + \bar{\beta}_{-} s^{\alpha_-} + \frac{s^{\alpha_R}}{\pi} \int_{-\infty}^{\alpha_c} \frac{\mathrm{Im} \, f(t,j)}{(j - \alpha_R)^2 + \alpha_I^2} \, dj + \frac{1}{\pi} \int_{-\infty}^{\alpha_c} \frac{\mathrm{Im} \, f(t,j) \, (s^j - s^{\alpha_R})}{(j - \alpha_R)^2 + \alpha_I^2} \, dj .$$

This is in a form relevant to the absorption model: it attempts to approximate the remaining integral by the explicit absorption model cut, in which the cut weight function is a smooth function of j. Obviously, this us a dubious procedure except in the limit $\alpha_I \to 0$; for any finite cut strength, i.e. for any finite α_I, the integrand is certainly not smooth. It appears, then, that the absorption model is likely to make sense only in the limit in which there is no cut at all.

Let us return now to the general form (3.3). Our discussion has made it evident what approximation we should make: we will assume that the function Im f(t,j) is relatively smooth over a range in j of the order of α_I around α_R. Then we may write

$$T(s,t) \approx \bar{\beta}_+ s^{\alpha_+} + \bar{\beta}_- s^{\alpha_-} + \frac{\mathrm{Im} f(t,\alpha_R)}{\pi} \int_{-\infty}^{\alpha_c} \frac{s^j}{(j-\alpha_R)^2 + \alpha_I^2}\, dj \quad . \qquad (3.4)$$

The similarity to the Breit-Wigner approximation is evident. There, one assumes that once one takes out a complex pole in the energy, the remaining weight function of the cut in the energy plane varies smoothly -- thus one ends up with a single complex pole in energy to describe the contributions of a cut in the energy.

Here we do exactly the same thing with j instead of energy, and a complex pair of poles instead of a single one.

The integral in Eq. (3.4) can be evaluated explicitly, and we find

$$T(s,t) = \bar{\beta}_+ s^{\alpha_+} + \bar{\beta}_- s^{\alpha_-} + \frac{\mathrm{Im} f(t,\alpha_R)}{2\pi i \alpha_I} \left[s^{\alpha_+} \bar{E}i(-\alpha_+ \log s) - s^{\alpha_-} \bar{E}i(-\alpha_- \log s) \right] \qquad (3.5)$$

The accuracy of this approximation depends, of course, on the function Im f, and on the size of α_I as well as on s. Representative examples are shown in Fig. 4. The Ei function has a simple representation:

$$Ei(-z) = \gamma + \log z + \sum_{n=1}^{\infty} \frac{(-z)^n}{n\, n!} \tag{3.6}$$

where γ is Evler's constant.

Using this representation, we may, if $|\alpha_{\pm} \log s| \lesssim 1$, finally express T as a pair of complex poles alone, in complete analogy to the Breit Wigner expression for an amplitude containing a resonance. We obtain

$$T(s,t) = \beta_+ s^{\alpha_+} + \beta_- s^{\alpha_-} \tag{3.7}$$

where

$$\beta_{\pm} = \bar{\beta}_{\pm} + \frac{(\phi \pm i(\gamma + \log R))\, \mathrm{Im}\, f(t, \alpha_R)}{2\pi \alpha_I} \,. \tag{3.8}$$

and we write $\alpha_+ - \alpha_c = R \exp i\phi$. Thus $\beta_+ = \beta_-^*$.

Again the error involved in replacing Eq. (3.5) by Eq. (3.7) depends, for a given s, on the size of α_I and of $(\alpha_R - \alpha_c) \log s$. An example is shown in Fig. 5. As before, for sufficiently large s, the approximation breaks down; but the smaller α_I, the farther it goes.

Because this stage of the approximations involves $(\alpha_R - \alpha_c) \log s$ as well as α_I, it should be noted that in some situations it may be more accurate to stop with Eq. (3.5), which is still an explicit form for the amplitude not involving detailed knowledge of the cut, and not to continue on to Eq. (3.7). Equation (3.5) requires only that α_I is small; Eq. (3.7) requires $|(\alpha_R - \alpha_c) \log s|$ to be small as well.

The essential assumption, leading to Eq. (3.4), was that Im f(t,j) had no unusual behaviour near $j = \alpha_R$. This assumption can be somewhat relaxed, without invalidating Eq. (3.8), as follows.

We expand Im f(t,j) in powers of j, around $j = \alpha_R$:

$$\mathrm{Im}\, f(t,j) = \sum_{n=0}^{\infty} a_n (j - \alpha_R)^n \,.$$

Inserting this expansion into the integral in Eq. (3.3) then yields

$$\sum_{n=c}^{\infty} a_n s^{\alpha_R} \left(s \frac{\partial}{\partial s} \right)^n \left(\frac{1}{\pi} \int_{-\infty}^{\alpha_c - \alpha_R} \frac{s^{J'}}{J'^2 + \alpha_I^2} \, dJ' \right) .$$

From this, in so far as the approximation of the Ei function we used before is valid, we readily again obtain Eq. (3.7), only now Eq. (3.8) is replaced by

$$\beta_\pm = \bar{\beta}_\pm + \frac{(\phi \mp i(\gamma + \log R)) \operatorname{Im} f(t, \alpha_\pm)}{2\pi \alpha_I} . \qquad (3.10)$$

We have, then, two somewhat complementary formulae. If Im f varies, but $|(\alpha_R - \alpha_c) \log s|$ is small, we may use Eq. (3.7). However, if Im f is smooth, but $|(\alpha_R - \alpha_c) \log s|$ is not so small, we can use Eq. (3.5). If both are valid, then of course we use Eq. (3.7).

In any event, subject to the stated assumptions, let us assume that we can obtain the form (3.7). The amplitude is thus described (to a high degree of accuracy over a sizeable range of s if α_I is fairly small) as a pair of complex conjugate Regge poles and nothing else. In this moderate energy range, the entire effect of the cut, no matter what the detailed behaviour of its discontinuity, looks just like the (Breit-Wigner like) complex pair of Regge poles. This, we emphasize, is true whether or not the poles lie on the physical sheet. The accuracy of the representation (or rather the range of s over which it is an accurate representation) depends on the size of α_I, and of $|(\alpha_R - \alpha_c) \log s|$; and it also depends on the smoothness of Im f in the vicinity of α_R. Finally, it is also important to note that the representation of the cut as a complex pair is far more accurate than to represent it simply by a single real pole -- that is, by the limiting case in which the cut is absent altogether.

The conclusion, then, is that the presence of a cut does not necessarily leave Regge theory with zero predictive power, even if very little is known about the cut. All that the cut accomplishes, in the moderate energy region at least, is to replace each real Regge pole which one would have dealt with in the absence of cuts, by a complex pair. The

number of parameters is therefore only doubled: whereas before, in a pure pole model, we had a real trajectory $\alpha(t)$ and a real residue $\beta(t)$ we now have a complex trajectory $\alpha(t) = \alpha_R(t) + i\,\alpha_I(t)$ and a complex residue $\beta(t) = |\beta(t)|\, e^{i\phi\beta(t)}$.

We may exhibit the correspondence to the single real pole explicitly. The amplitude of Eq. (3.7), for a complex pair of poles, may be written in the following simple form: (we now re-introduce the signature).

For even signature

$$T(s,t) = \gamma_+ s^{\alpha_+} e^{-i\pi\alpha_+/2} + \gamma_- s^{\alpha_-} e^{-i\pi\alpha_-/2}$$

$$= |\gamma|\, s^{\alpha_R} e^{-i\pi\alpha_R/2} \times F(s,t) \qquad (3.11)$$

where the "correction factor" F is

$$F(s,t) = \cos(\alpha_I \log s + \varphi_\gamma) \cosh \pi\alpha_I/2 + i \sin(\alpha_I \log s + \varphi_\gamma) \sinh \pi\alpha_I/2 \qquad (3.12)$$

For odd signature

$$T(s,t) = i\,|\gamma|\, s^{\alpha_R} e^{-i\pi\alpha_R/2} \times F(s,t) \qquad (3.13)$$

with the same "correction factor" F.

It should always be kepd in mind that this correction factor only represents, approximately, the existence of the cut. For that reason the residues in Eqs. (3.11) and (3.13) do not factor. Only the residue of a true pole factors; the complex "poles" we deal with here are not really poles of the partial wave amplitude (though they may include con-

tributions from physical sheet poles if there are any) but are only approximations to a cut.

For the same reason it is possible for the complex poles alone to produce polarization; this simply reflects the fact that a cut can produce polarization. Again, complex poles can produce "cross-over zeros" without the residue vanishing; (this can happen because F vanishes, not $|\beta|$). This is merely saying that a cut can give a cross-over zero. And so forth.

We have now completed our theoretical development. The result we have obtained is that if the cut is fairly weak, so that α_I is small, then even though nothing is known about the cut there are nevertheless phenomenological predictions. Indeed, an entire Regge pole plus Regge cut combination, up to some cut-off energy (the weaker the cut the higher the cut-off) is describable to a high degree of accuracy by only a complex conjugate pair of poles, and nothing else.

The following section will be devoted to some detailed illustrations of the use of this result in specific phenomenological situations, to conclude this section, however, let us make a few general observations, as follows.

3.1 Total cross-sections

As we have seen, the contribution of a given complex Regge pair of even signature to the imaginary part of a forward elastic amplitude will be

$$+ |\gamma(0)| \, s^{\alpha_R(0)} \, \mathrm{Im}\left(\epsilon^{-i\pi\alpha_R(0)/2} F(s,0) \right) \tag{3.14}$$

(For odd signature, an extra factor of i is inserted in the bracket). Using the form given for F in Eq. (3.12), this may be rewritten as a contribution to the total cross-section of

$$|\gamma(0)| \, s^{\alpha_R(0)-1} \left\{ \cos\left(\alpha_I(0)\log s + \varphi_\gamma(0)\right) \sin\tfrac{\pi\alpha_R}{2} \cosh\tfrac{\pi\alpha_I}{2} - \sin\left(\alpha_I(0)\log s + \varphi_\gamma(0)\right) \cos\tfrac{\pi\alpha_R}{2} \sinh\tfrac{\pi\alpha_I}{2} \right\}. \tag{3.15}$$

At first sight, therefore, there would appear to be an oscillation with increasing log s, of period $2\pi/\alpha_I(0)$, assuming that $\alpha_I(0) = 0$ [12]. Several cautionary remarks are, however, necessary[13]. First, the approximation of replacing the cut by a complex pair failed when s became sufficiently large; in fact by referring back to the original integral for the cut, Eq. (3.5), it is easily seen that it necessarily fails before the oscillations in Eq. (4.2) begin. The cut term actually goes monotonically down, and does not oscillate at all. Oscillations can exist only if there are physical sheet complex poles (i.e. if $\bar{\beta}_\pm \neq 0$).

Secondly, while oscillatory terms, if they exist, do not cause any trouble for lower lying Regge poles (for which $\alpha_R(0) < 1$) it is obviously not possible for the Pomeranchon itself to exhibit such behaviour; if it did, we would eventually find negative total cross-sections. For the Pomeranchon, therefore (if it is also describable, at least approximately, as a complex pair) either $\alpha_I(0) = 0$ or the complex pole is on an unphysical sheet.

3.2 Forward Diffraction peaks

The question of how the complex pole idea applies to the Pomeranchon may as well be faced immediately, since it's been brought up in the context of total cross-sections. Let us list the possibilities.

i) The Pomeranchon is simply a real pole -- perhaps like the physical sheet pole in the logarithmic cut model[14]. In this event the total cross-section is the normal Pomeron contribution plus, perhaps, damped oscillatory contributions from lower lying complex pairs.

ii) The Pomeranchon is a complex pair, either with $\alpha_I(0) = 0$ or on an unphysical sheet to avoid negative cross-sections. In this event, we can see from Eq. (3.11) that an elastic differential cross-section looks like

$$d\sigma/dt = \left(d\sigma/dt\right)_{\alpha_I = 0} |F(s,t)|^2$$

and we note

$$|F(s,t)|^2 = 1 + \sinh^2 \pi \alpha_I/2 - \sin^2 (\alpha_I \log s + \varphi_r)$$

The correction factor thus introduces minima in $d\sigma/dt$ which move toward $t = 0$ with $\log s$ [15].

iii) The Pomeranchon is something entirely different. The entire question of what constitutes diffraction scattering has, of course, always been present in Regge theory. We do not escape the uncertainty here; as a result, detailed phenomenological analysis of elastic processes where Pomerons exist, are subject to some ambiguity.

4. APPLICATIONS

4.1 π-N charge exchange scattering[16)]

We shall begin with this reaction for the usual reasons: it is rather well measured, and, more important, it is theoretically very clean because only a single important trajectory, the ρ, can be exchanged.

There are two scalar amplitudes in this process, the usual $A'^{(-)}$ and $B^{(-)}$. In conformity with the foregoing discussion, these are parametrized by a single pair of complex poles, representing the ρ trajectory and its associated cut. We write

$$A'^{(-)} = \gamma'_{+A}\left(\frac{1-e^{-i\pi\alpha_+}}{\sin\pi\alpha_+}\right)\left(s/s_0\right)^{\alpha_+} + \gamma'_{-A}\left(\frac{1-e^{-i\pi\alpha_-}}{\sin\pi\alpha_-}\right)\left(s/s_0\right)^{\alpha_-} \tag{4.1}$$

and

$$B^{(-)} = \alpha_+\gamma_{+B}\left(\frac{1-e^{-i\pi\alpha_+}}{\sin\pi\alpha_+}\right)\left(s/s_0\right)^{\alpha_+-1} + \alpha_-\gamma_{-B}\left(\frac{1-e^{-i\pi\alpha_-}}{\sin\pi\alpha_-}\right)\left(s/s_0\right)^{\alpha_--1} \tag{4.2}$$

The factors α_+ and α_- in the residues of the B amplitude are conventional and reflect the P'_ℓ appearing in the cross channel partial wave expansion for B.

For α_R the usual straight line trajectory is chosen: $\alpha_R(t) = a + bt$; we expect that as in the simple real pole situation we will find $a \sim 0.5$ and $b \sim 1.0$.

Two models are chosen for α_I, corresponding (roughly) to the square root and log cases. We try both $\alpha_I(t) = g\sqrt{-t}$ and $\alpha_I(t) = g$ (a constant).

Finally, for the residues we choose forms similar to the normal ones; specifically $\gamma_{+A} = h_0\, e^{h_1 t}(\alpha_+ + 1)\, e^{i\phi_{+A}}$ and $\gamma_{+B} = d_0\, e^{d_1 t}(\alpha_+ + 1)\, e^{i\phi_{+B}}$. (Of course $\gamma_{-A} = \gamma^*_{+A}$ and $\gamma_{-B} = \gamma^*_{+B}$.) The phases are parametrized by either $\phi_{+A} = \pi\sqrt{-t}(\gamma_0 \mp \gamma_1 t)$ or by $\phi_{+A} = \pi(\gamma_0 + \gamma_1 t)$ corresponding to the two choices for α_I, with similar expressions for ϕ_{+B}.

There are two manifestations of the complex poles to look for, neither of which can be understood with a real ρ pole alone. These are polarization and the cross-over phenomenon. Only these allow us to fix α_I and the phases; the remaining data, on $d\sigma/dt$ and $\sigma_T(\pi^- p) - \sigma_T(\pi^+ p)$, provide only negative constraints, in that the excellent fits to these which can be obtained with a real pole alone must not be seriously disturbed.

Results for all this are shown in Figs. 6 and 7, and the corresponding parameters are listed in reference 16, for the "square root" and "constant" models of α_I mentioned earlier. The best fit trajectories in the two cases are

$$\alpha^{\rho}_{\pm}(t) = 0.53 + 1.02 \pm 0.20\, i\sqrt{-t} \qquad (4.3)$$

and

$$\alpha^{\rho}_{\pm}(t) = 0.50 + 0.95\, t \pm 0.088\, i \,. \qquad (4.4)$$

The fits are excellent, though of course the miserable quality of the polarization data precludes us from a serious test of the forms of α_I. It may be noted, also, that a cross-over is indeed obtained; however, its position is not sensitive to the parameters and may be placed anywhere in the range $t = -0.15$ (GeV)^2 to $t = -0.5$ (GeV)^2 without affecting the other fits.

4.2 π-N Backward Scattering[17)]

We limit ourselves here to two trajectories, the N and the Δ, and confine our attention, for the time being, to the "square root" model. Fits are made to backward differential cross-sections for the three processes $\pi^- p \to p\pi^-$, $\pi^+ p \to p\pi^+$ and $\pi^- p \to n\pi^0$.

There are, now, many parameters (22 to be exact). Best fits are shown in Figs. 8, 9 and 10, and the corresponding trajectories are, for the nucleon,

$$\alpha_{\pm}^{N}(w) = -0.42 - 0.03w + 0.54w^2 \pm 1.04w\sqrt{0.27w^2 - 0.03w + 0.04} \tag{4.5}$$

and for the Δ

$$\alpha_{\pm}^{\Delta}(w) = 0.07 + 0.08w + 0.44w^2 \pm 0.94w\sqrt{0.22w^2 + 0.08w - 0.05} \tag{4.6}$$

Points to be emphasized are that one can obtain excellent fits to the dip in backward charge exchange scattering, and that the trajectories given in Eqs. (4.5) and (4.6) have no MacDowell partners.

4.3 π-N Elastic Scattering

As yet results for these processes do not exist. When they do, they will be plagued by the uncertainty, already referred to at the end of Section 3, arising from the Pomeron. The most straightforward thing to do is simply to permit the Pomeron to be a complex pair as well, and see what happens; this is what is being done in the fits to forward π-N elastic scattering. (As mentioned before, there are of course some constraints on the Pomeron; for example, if it is on the physical sheet, it must have $\alpha_I = 0$ at $t = 0$. These constraints do not seriously affect the data fitting, however.)

4.4 Other pseudoscalar meson-baryon scattering processes: Line reversal

Next we discuss processes such as K-N scattering, and hyperon production in K-N or π-N collisions.

One thing to be done here is, of course, simply to make detailed fits in complete analogy to those we have already discussed for π-N scattering. Before going on to do this, however, some more general comments are in order, having to do with the relation of exotic processes and their line reversed associates[18]. As examples, think of the exotic charge exchange process $K^+n \to K^0p$ and its line reversed partner $\bar{K}^0n \to K^-p$, or the exotic hypercharge exchange process $K^-p \to \pi^-\Sigma^+$ together with its line reversed associate $\pi^+p \to K^+\Sigma^+$.

It is, apparently, experimentally the fact that the ratio R(s,t) of an exotic differential cross-section to the differential cross-section of its line reversed partner is always greater than one[19]. It is also quite difficult to understand this fact within pure Regge pole models, and even within Regge models containing absorptive cuts. The point is that the reality of exotic amplitudes requires, through duality, exchange degeneracy of the Regge trajectories contributing to the high energy form of the amplitude (ρ-A_2 for charge exchange, and K^*-K^{**} for hypercharge exchange); indeed, this exchange degeneracy seems well confirmed experimentally, at least in some cases[20]. But, with exchange degeneracy, a pure pole model yields $R(s,t) \equiv 1$, and including absorptive cuts gives $R(s,t) < 1$.

This apparent difficulty is easily resolved when one replaces the (incorrect) absorptive cut model by the more realistic complex pole picture. With exact exchange degeneracy, we may write for the exotic amplitude the representation

$$T_E(s,t) = \frac{1}{\pi}\int_{-\infty}^{\alpha_L} \frac{\mathrm{Im}\, f(t,j)\, s^j}{(j-\alpha_+)(j-\alpha_-)}\, dj$$

as in Eq. (3.3). (We assume the complex pole to be on the unphysical sheet, for now.) For the line-reversed non-exotic amplitude, we obtain, in contrast

$$T_N(s,t) = \frac{1}{\pi}\int_{-\infty}^{\alpha_L} \frac{\mathrm{Im}\, f(t,j)\, s^j\, e^{-i\pi j}}{(j-\alpha_+)(j-\alpha_-)}\, dj$$

with the same weight function Im f. Now, obviously, if Im f is smoothly varying around α_R over a region of j of order α_I, we get $|T_N| < |T_E|$, and hence find $R(s,t) > 1$.

Detailed fits to the (relatively poor) data on R(s,t) for both Σ and Λ production (the pairs $K^-p \to \pi^-\Sigma^+$ and $\pi^+p \to K^+\Sigma^+$, and $K^-n \to \pi^-\Lambda$ and $\pi^-p \to K^0\Lambda$) can be made, and these provide adequate fits to the (also poor) polarization data available as well[18]. The resulting exchange degenerate K^*-K^{**} trajectory is either (square root case)

$$\alpha_{\pm}^{K^*}(t) = 0.4 + 1.0\,t \pm 0.6\, i\sqrt{-t} \qquad (4.7)$$

or (constant case)

$$\alpha^{K^*}_{\pm}(t) = 0.4 + 1.0\,t \pm 0.2i\,(1-2t) \,. \qquad (4.8)$$

It is interesting to note that the α_I for the K^*-K^{**} is noticeably larger than that for the ρ-A_2 found earlier; this is quite consistent with the fact that R(s,t) for charge exchange is smaller than for hypercharge exchange, and tends to decrease more rapidly toward one as the energy increases.

As to detailed fits to, for example, K-N data, these have not yet been done. Obviously it will be interesting to see how these work, in order to check that the same α_I for the ρ as we obtained before works here too.

4.5 Baryon-Baryon scattering

Here, as yet, no fits exist; however, a fit to the n-p CEX scattering is under way, and hopefully, will be available soon[21].

4.6 Vector-meson production

The only fit existing so far under this heading is a fit to the reaction $\pi^+ p \to \pi^0 \Delta^{++}$ [22]. This reaction is a natural one to choose, since one believes that it, like π-N CEX is dominated by ρ exchange alone; it should therefore provide another check on the ρ-parameters found earlier.

Unfortunately, the functional form chosen here for $\alpha_I(t)$ is not quite identical to either the "square root" or "constant" models; however, it is not too different from the "constant" case. The best fit turns out to give

$$\alpha^{\rho}_{\pm}(t) = 0.57 + 0.96\,t \pm \frac{0.274\,i}{1.14 - t} \,. \qquad (4.9)$$

For very small t, we have here an $\alpha_I = 0.24$ while in the "constant" case before we got $\alpha_I = 0.09$. It is not clear whether this is or is not a serious discrepancy; perhaps it is to be attributed to the different choice of functional forms, and to different choices of the other parameters. Fits obtained to $d\sigma/dt$ and to the spin density matrix elements are shown in Figs. 11 and 12.

4.7 Photoproduction

One fit, so far, exists here[23], to near forward charged pion photoproduction. The dominant trajectories are assumed to be the pion and the A_2. Fits are made to the differential cross-section and to the asymmetry parameters for pion production by linearly polarized photons on polarized nucleons. Best fits are shown in Figs. 13, 14 and 15; the corresponding trajectories are

$$\alpha^{\pi}_{\pm}(t) = -0.02 + 1.0\,t \pm 1.03\,i \tag{4.10}$$

and

$$\alpha^{A_2}_{\pm}(t) = 0.25 + 1.0\,t\,. \tag{4.11}$$

The results are quite insensitive to the A_2; the pion plays by far the dominant role. For this reason an α_I for the A_2 has been ignored.

The value of α_I for the pion seems abnormally large, in comparison with those found earlier for other trajectories. Indeed, one is entitled to wonder whether, with such a large α_I the entire approximation of replacing the pole-cut combination with simply a complex pair of poles is not invalidated. For this reason it is worth noting explicitly that the residue functions in this fit are explicitly assumed to be real; the phases ϕ_β are set equal to zero. It may well be that if this (somewhat artificial) constraint is relaxed, a smaller α_I, more in keeping with our earlier results, will be obtained.

REFERENCES AND FOOTNOTES

1) S. Mandelstam, Nuovo Cimento 30, 1127 (1963).

2) R. Eden et al., "The Analytic S-matrix" (Cambridge Univ. Press, 1966).

3) R. Carlitz and M. Kislinger, Phys. Rev. Letters 24, 186 (1970). It should be emphasized that the cut occurring in this model may well be the same as that suggested by Mandelstam (ref. 1). For example, if $\alpha_p(t) = 1$, then the first Mandelstam cut is also flat and crosses the pole at $t = 0$. Or, the identification may be more subtle. It might be that the C-K cut coincides with the ultimate Mandelstam cut which is, perhaps, flat. Or it might be that the C-K cut is not really flat, but only appears so in the simple model in which they first obtained it. In any case it is highly unattractive to believe that the C-K and Mandelstam cuts really represent different phenomena.

4) In fact, we shall show that the specific values for the cut discontinuities assumed in these models are unlikely ever to be correct. Thus all cut models in use so far are, in fact, wrong. The predictions of such models may be specific; they are also wrong.

5) The partial wave amplitude is of a given signature. It should be emphasized that we presume there to be a cut, of the same quantum numbers and the same signature, associated with each Regge pole of a given signature. Generally, however, the signature is merely a notational complication; we shall therefore normally ignore it, and mention it only where its inclusion is not entirely obvious or where it makes some important difference.

6) Evidently, D_c is not uniquely defined by Eq. (2.1). The following examples illustrate what is meant by it.

7) In order to keep N real on the right-hand cut, α_{in} must be a polynomial in t, which we take to be linear. In order to assure that α_{out} is a zero of D, and not a pole of N, N and D are both multiplied by $(j - \alpha_{in})$; this, of course, does not alter their analyticity properties.

8) Hung Cheng, Phys. Rev. 130, 1283 (1963).

9) P. Kaus and F. Zachariasen, Phys. Rev. D1, 2962 (1970).

10) W.R. Frazer and C.M. Mehta, Phys. Rev. D1, 696 (1970).
J.S. Ball and G. Marchesini, Phys. Rev. 188, 2508 (1969).
G.F. Chew and D.R. Snider, UCRL 20033, July 1970.

11) J.S. Ball, G. Marchesini and F. Zachariasen, Phys. Letters 31 B, 583 (1970).

12) G. Chew and D. Snider, Phys. Letters 31 B, 71 (1970). It should be noted that the model which these authors base their discussion on has a logarithmic cut; the complex poles are therefore always on unphysical sheets. Hence oscillating terms, the total cross-sections cannot occur.

13) See Ref. 11.

14) See G.F. Chew and D.R. Snider (Ref. 10). They interpret the physical sheet pole in a logarithmic cut model as the Pomeron, and the nearest unphysical sheet complex pair as the P'.

15) The suggestion that the Pomeron is a complex pair was made first by Freund and Oehme, Phys. Rev. Letters 10, 459 (1963). They suggest, in addition, that $\alpha_P = 1$, a constant, for the Pomeron, in an attempt to have (nearly) non shrinking diffraction peaks without violating t-channel unitarity.

16) B.R. Desai, P.E. Kaus, R.T. Park and F. Zachariasen, Phys. Rev. Letters 25, 1389 (1970).

17) R.T. Park and P.E. Kaus, private communication.

18) D.P. Roy, J. Kwiecinski, B.R. Desai and F. Zachariasen, to be published.

19) K. Lai and J. Louie, Nuclear Phys. B19, 205 (1970).

20) A. Firestone et al., Phys. Rev. Letters 25, 958 (1970).

21) D.P. Roy, private communication.

22) P. Butero, M. Enriotti and G. Marchesini, University of Milan preprint, December (1970).

23) J.S. Ball, H.J.W. Müller and B.K. Pal, preprint UCRL 20057, August (1970).

Figure captions

Fig. 1a : A trajectory, and the sequence of branch points generated by its repeated interference with the Pomeron, if $\alpha_p(0) = 1$.

1b : A trajectory, and the sequence of branch points generated by its repeated interference with the Pomeron, if $\alpha_p(0) < 1$.

Fig. 2 : The unperturbed or input trajectory, the branch point, and the output physical and first sheet poles, in a logarithmic cut model.

Fig. 3 : The unperturbed or input trajectory, the branch point, and the two output trajectories, in a square root cut model.

Fig. 4a : Comparison of Eqs. (3.3) and (3.5) in a square root cut model. For $\alpha_c - \alpha_R = -0.3$, $\alpha_I = 0.2$ and Im $f = \sqrt{-\ell}$. (From Ref. 11).

4b : Comparison of Eqs. (3.3) and (3.5) in a logarithmic cut model, so that Im $f = (\ell - \alpha_+)(\ell - \alpha_-)/(\ell - \alpha_0 - g \log(-\ell))^2 + \pi^2 g^2$ with $g = 0.05$ and $\alpha_0 = -0.35$. (From Ref. 11).

Fig. 5 : Comparison of Eqs. (3.5) and (3.7), for $\alpha_c - \alpha_R = -0.3$, $\alpha_I = 0.2$.

Fig. 6 : Fits to π-N CEX data for the "square root" model. (From Ref. 16).

Fig. 7 : Fits to π-N CEX data for the "constant" model. (From Ref. 16).

Fig. 8 : Fits to $d\sigma/dt$ for $\pi^+ p \to p\pi^+$. (From Ref. 17).

Fig. 9 : Fits to $d\sigma/dt$ for $\pi^- p \to p\pi^-$. (From Ref. 17).

Fig. 10 : Fits to $d\sigma/dt$ for $\pi^- p \to n\pi^0$. (From Ref. 17).

Fig. 11 : Fits to $d\sigma/dt$ for $\pi^+ p \to p^0 \Delta^{++}$. (From Ref. 22).

Fig. 12 : Fits to density matrix element for $\pi^+ p \to p^0 \Delta^{++}$. (From Ref. 22).

Fig. 13 : Fits to $d\sigma/dt$ for $\gamma p \to \pi^+ n$. (From Ref. 23).

Fig. 14 : Fit (solid line) to polarized photon asymmetry parameter The dotted line shows the perturbation theory prediction. (From Ref. 23).

Fig. 15 : Fit to left-right asymmetry parameter A. (From Ref. 23).

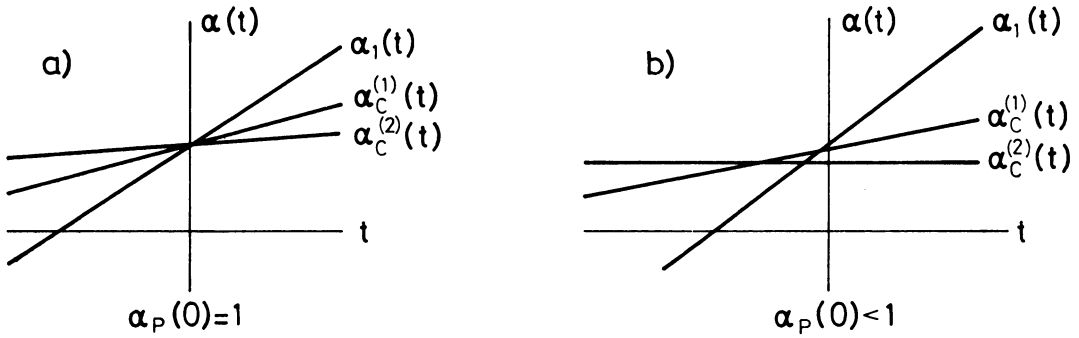

Fig. 1

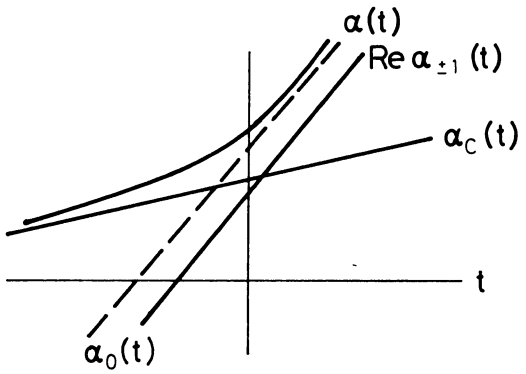

Fig. 2

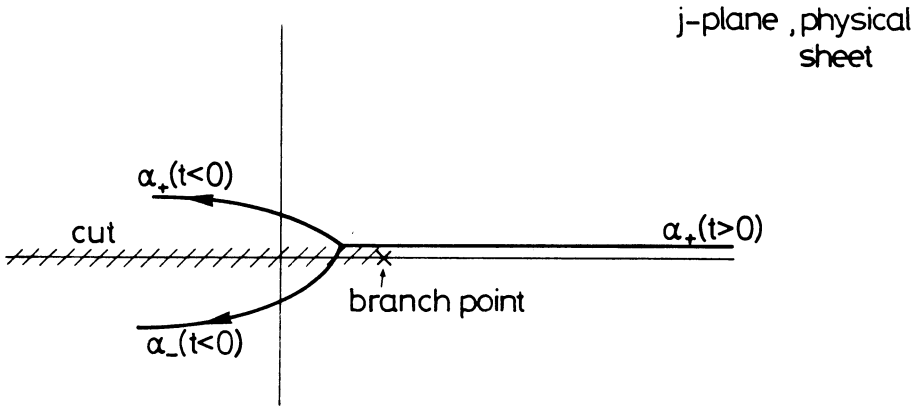

Fig. 3

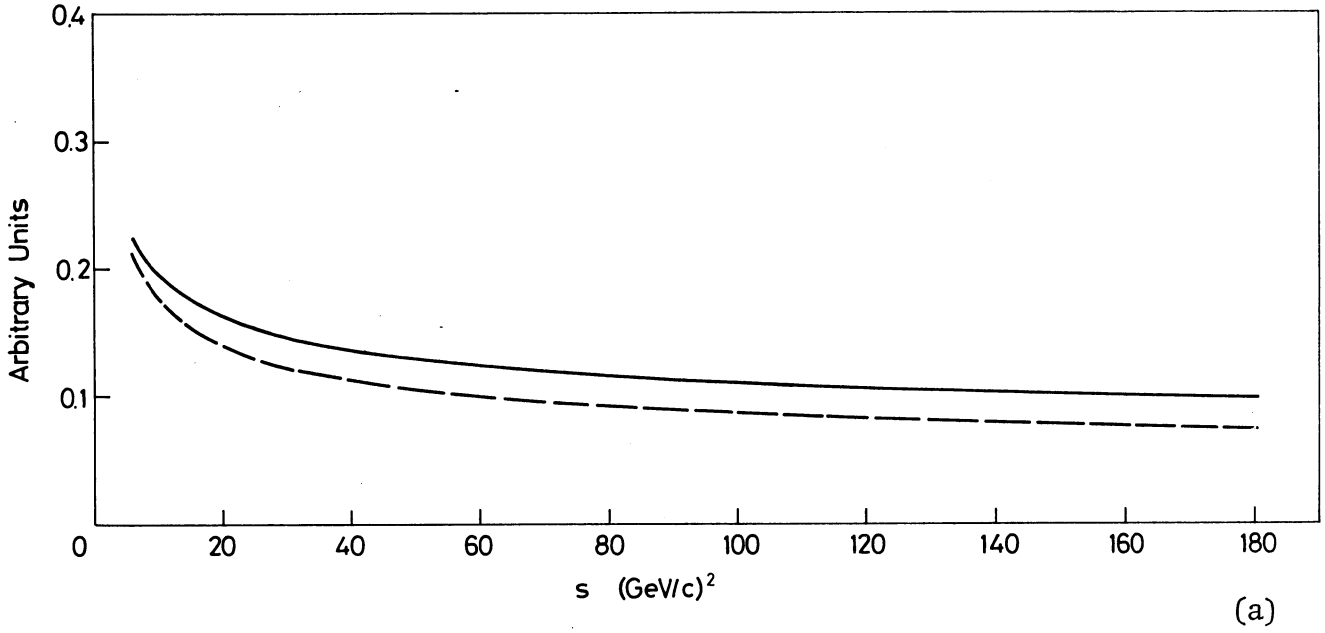
0.4
0.3
0.2
0.1
0
Arbitrary Units
20
40
60
80
100
120
140
160
180
s (GeV/c)²

(a)

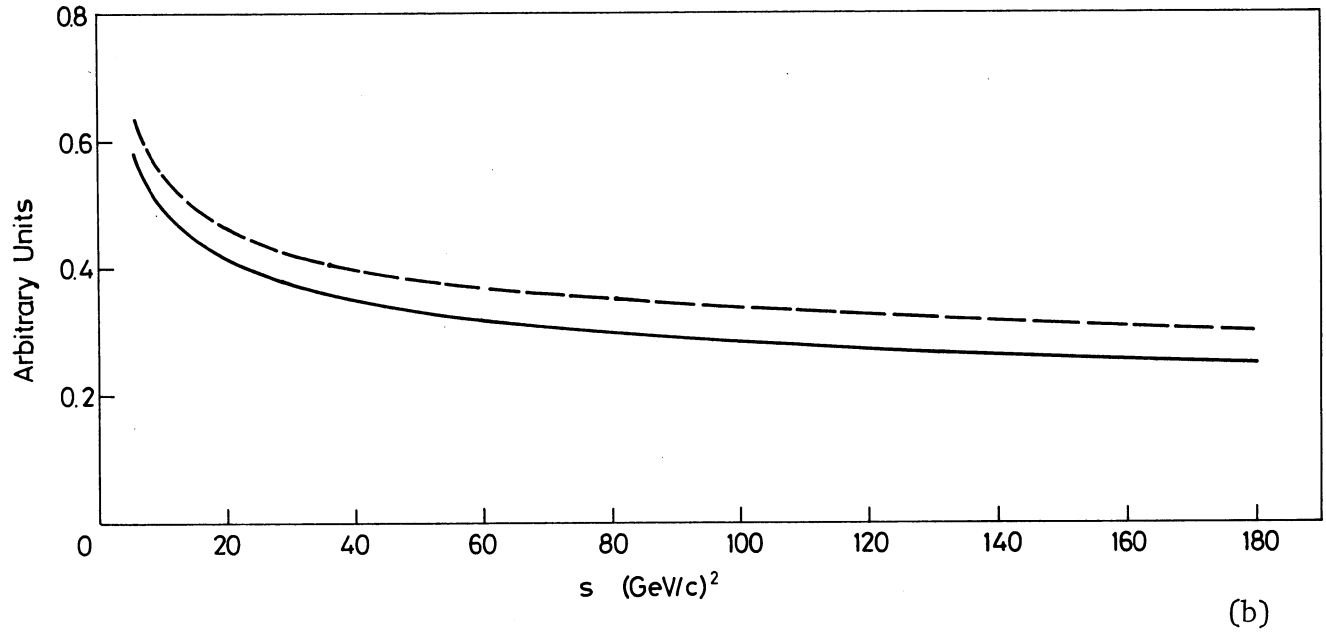
0.8
0.6
0.4
0.2
0
Arbitrary Units
20
40
60
80
100
120
140
160
180
s (GeV/c)²

(b)

Fig. 4

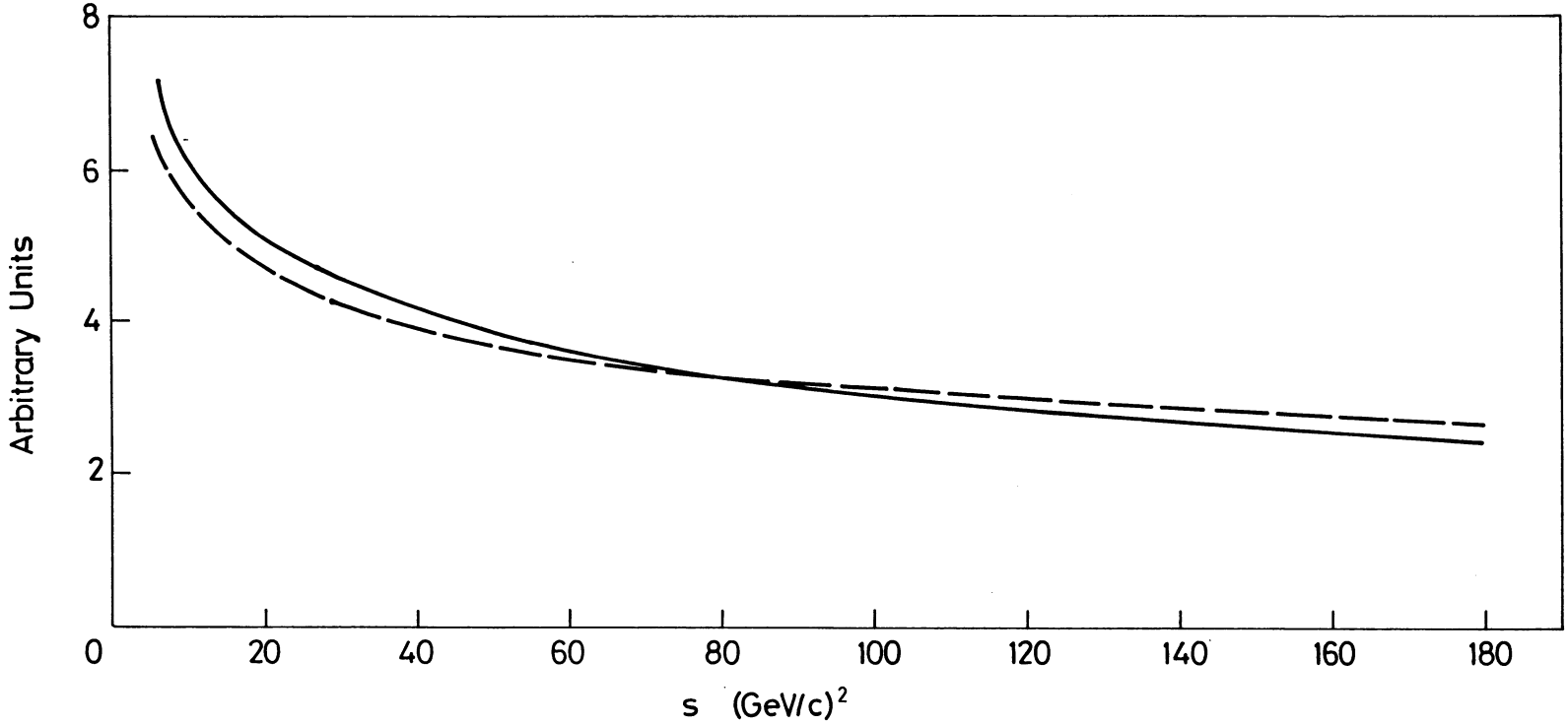

Fig. 5

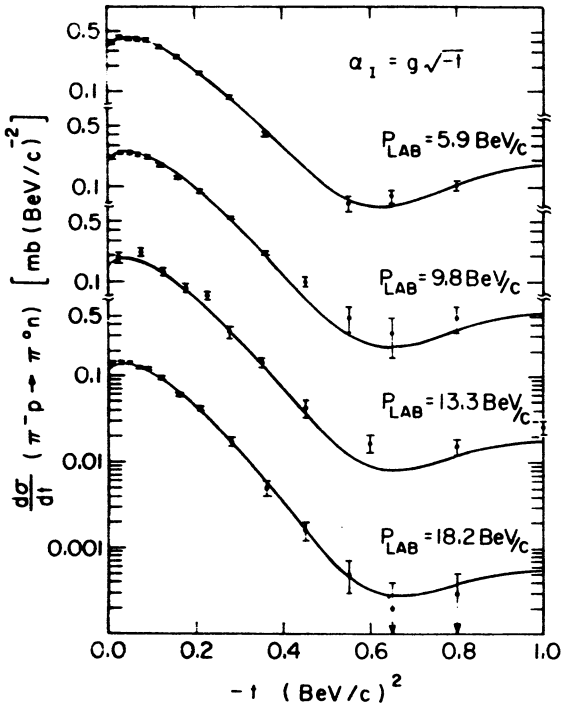
$\alpha_I = g\sqrt{-t}$
P_{LAB} = 5.9 BeV/c
P_{LAB} = 9.8 BeV/c
P_{LAB} = 13.3 BeV/c
P_{LAB} = 18.2 BeV/c
$\frac{d\sigma}{dt}$ ($\pi^- p \to \pi^0 n$) [mb (BeV/c)$^{-2}$]
$-t$ (BeV/c)^2

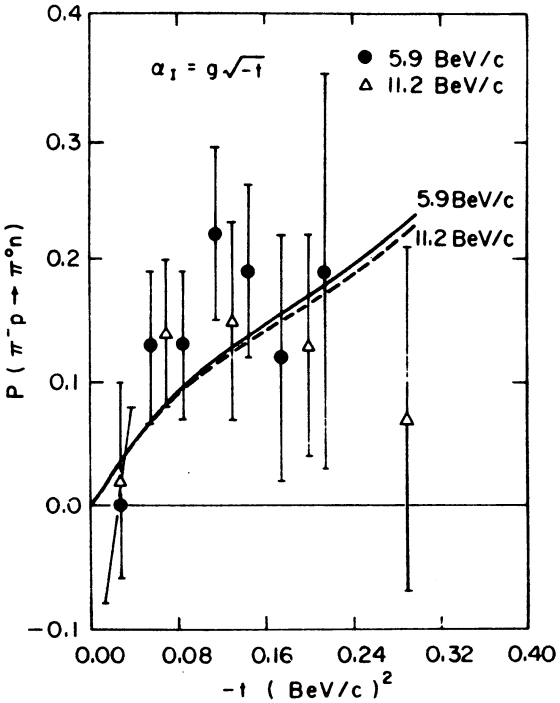
$\alpha_I = g\sqrt{-t}$
5.9 BeV/c
11.2 BeV/c
5.9BeV/c
11.2 BeV/c
P ($\pi^- p \to \pi^0 n$)
$-t$ (BeV/c)^2

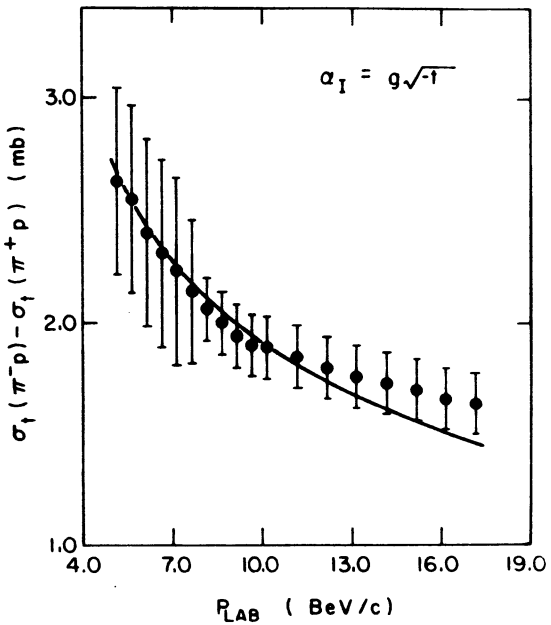
$\alpha_I = g\sqrt{-t}$
σ_t ($\pi^- p$) − σ_t ($\pi^+ p$) (mb)
P_{LAB} (BeV/c)

Fig. 6

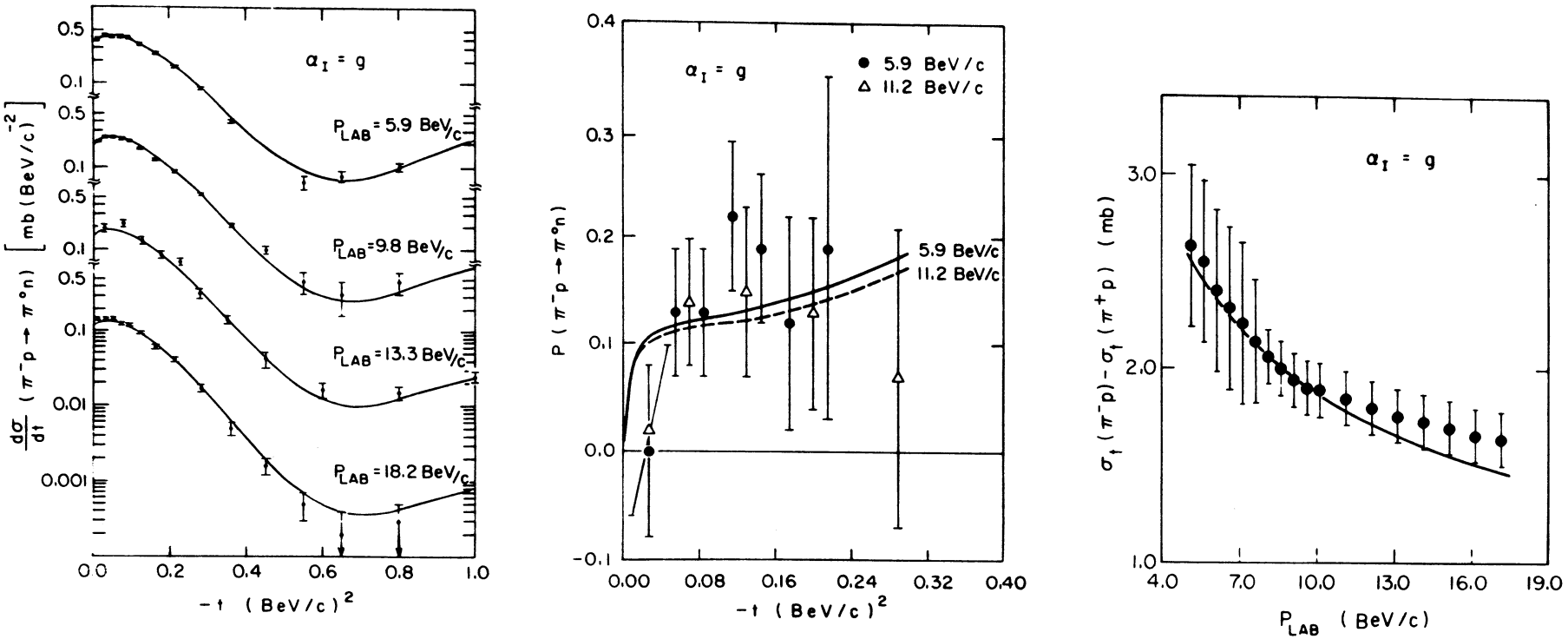
α_I = g
P_{LAB} = 5.9 BeV/c
P_{LAB} = 9.8 BeV/c
P_{LAB} = 13.3 BeV/c
P_{LAB} = 18.2 BeV/c
$\frac{d\sigma}{dt}$ ($\pi^- p \to \pi^0 n$) [mb (BeV/c)$^{-2}$]
$-t$ (BeV/c)^2
α_I = g
5.9 BeV/c
11.2 BeV/c
P ($\pi^- p \to \pi^0 n$)
5.9 BeV/c
11.2 BeV/c
$-t$ (BeV/c)^2
α_I = g
σ_t ($\pi^- p$) - σ_t ($\pi^+ p$) (mb)
P_{LAB} (BeV/c)

Fig. 7

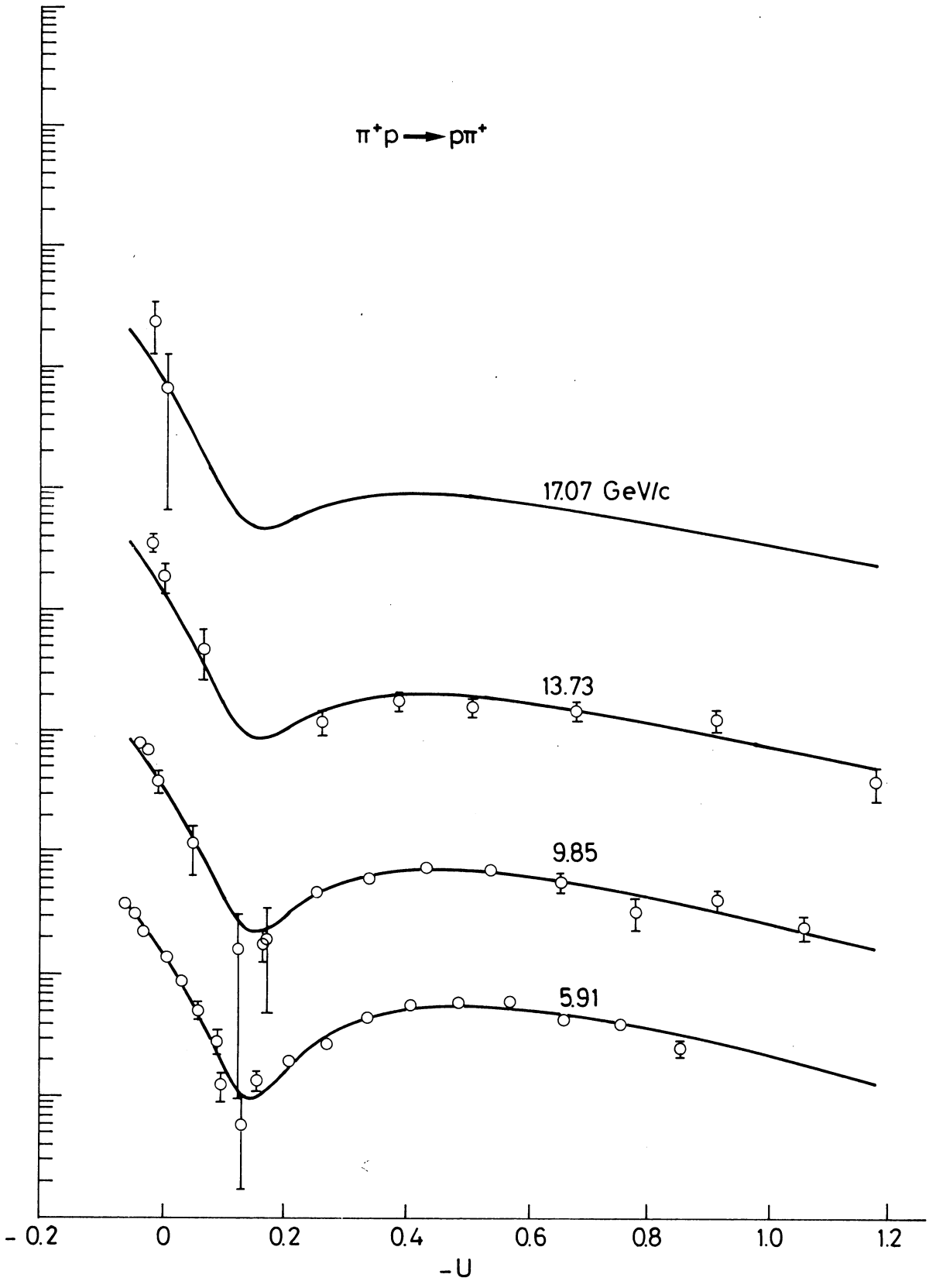

Fig. 8

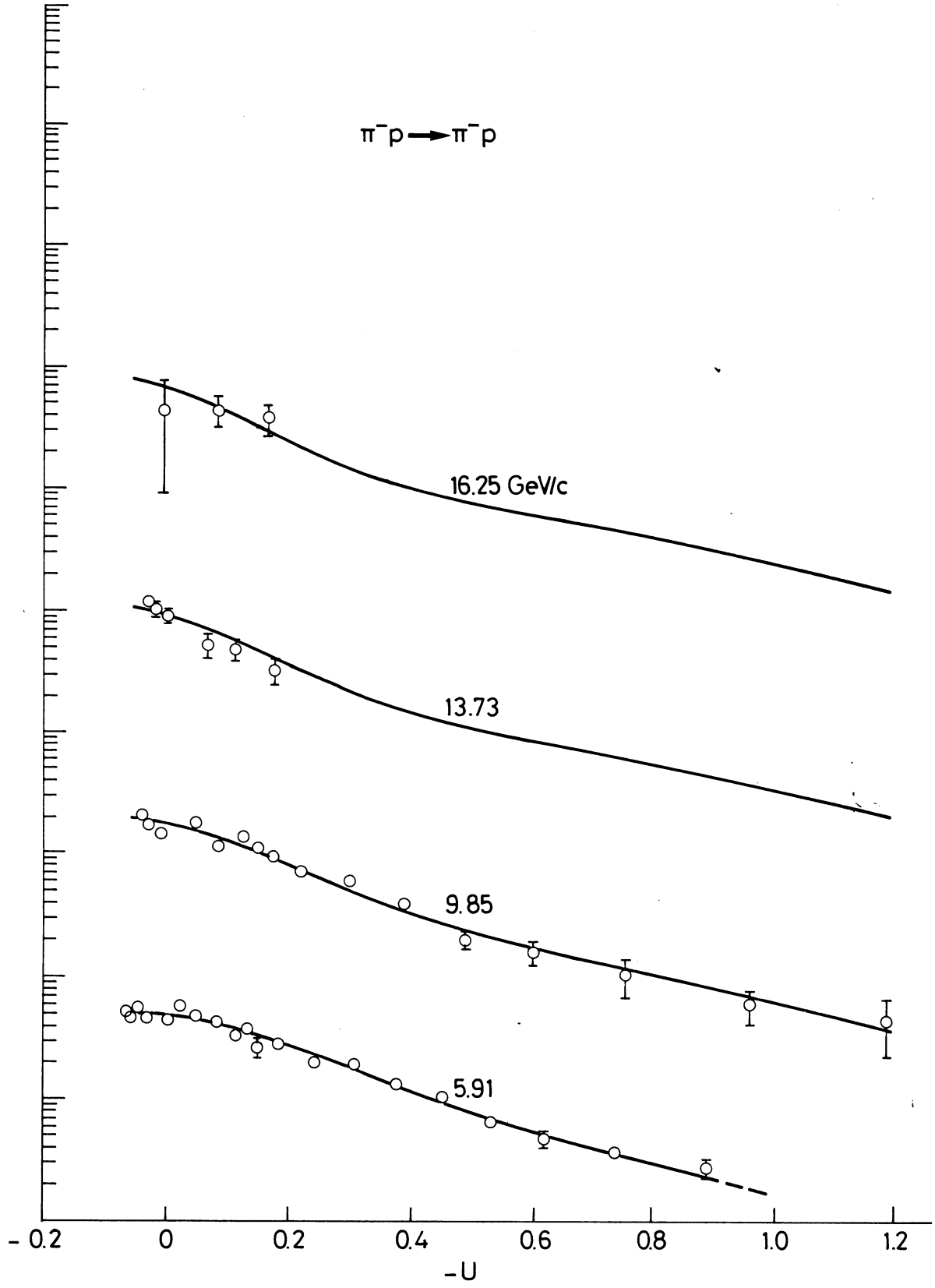

Fig. 9

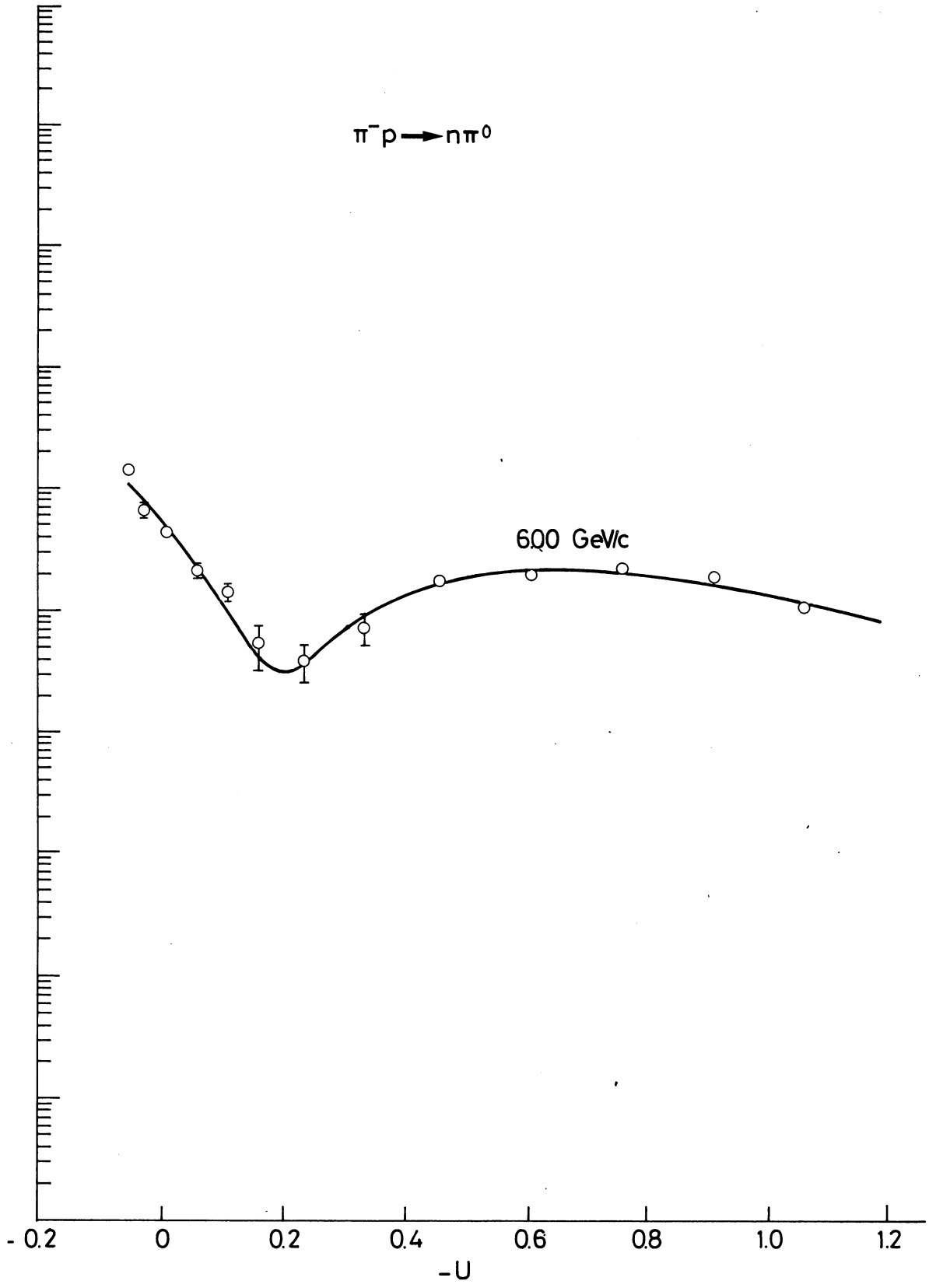

Fig. 10

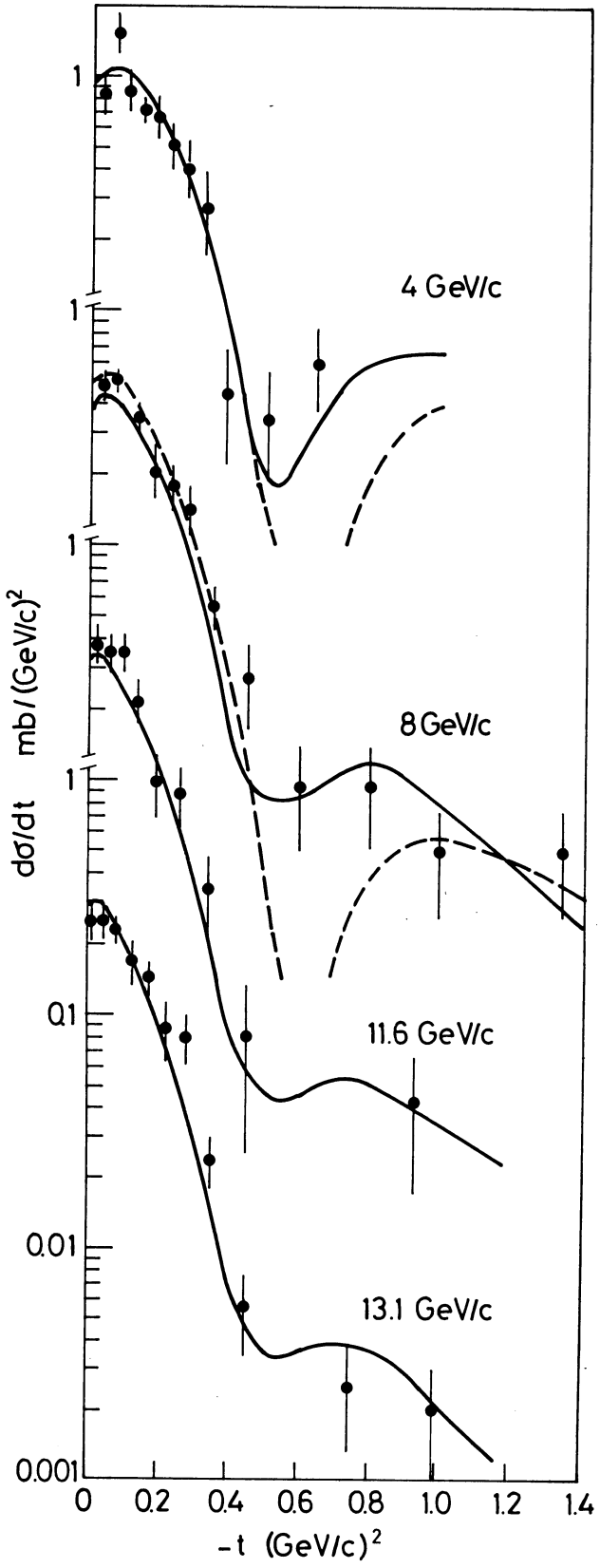
4 GeV/c
8 GeV/c
11.6 GeV/c
13.1 GeV/c
dσ/dt mb/(GeV/c)²
-t (GeV/c)²
1
1
1
1
0.1
0.01
0.001
0
0.2
0.4
0.6
0.8
1.0
1.2
1.4

Fig. 11

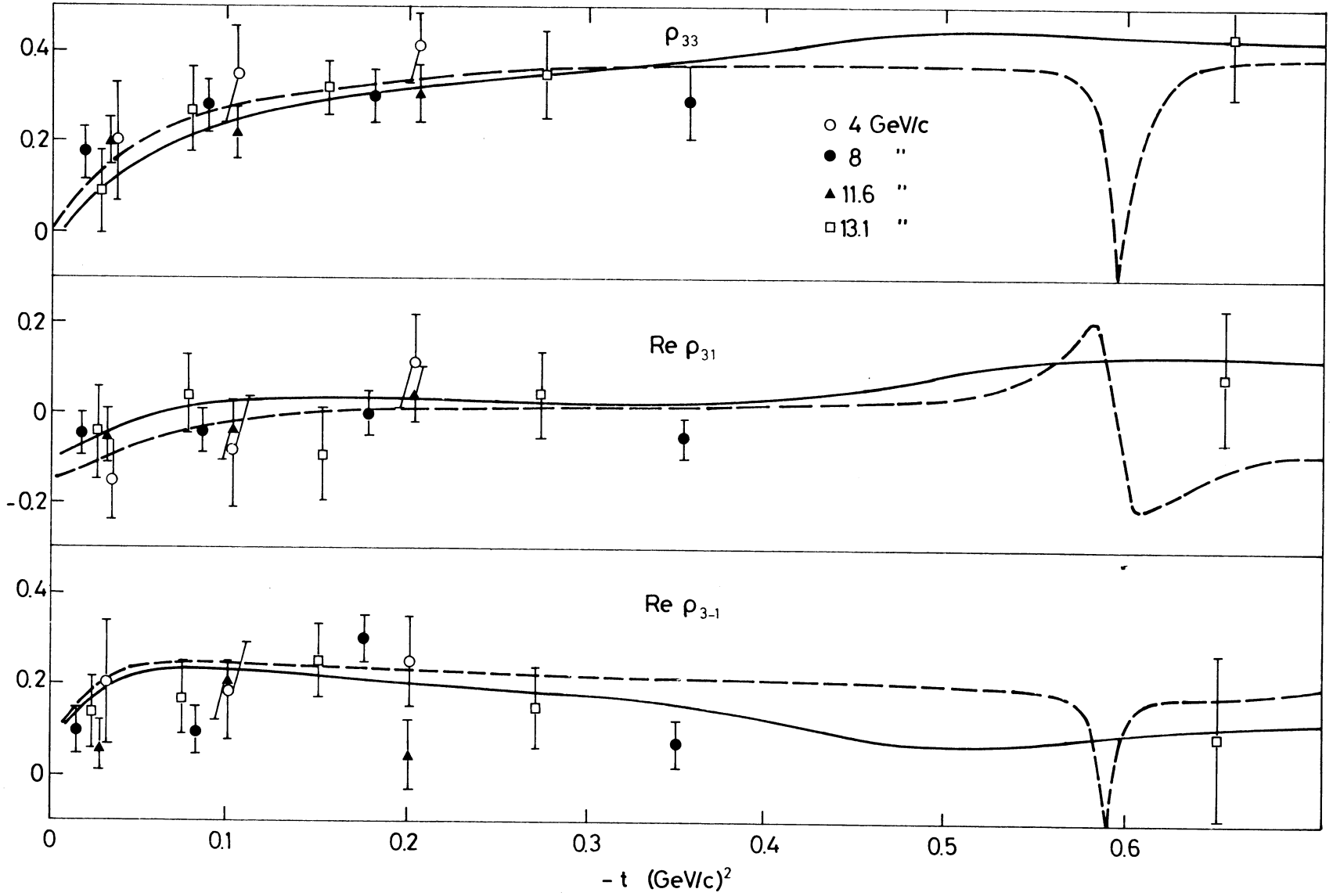
ρ_{33}
○ 4 GeV/c
● 8 "
▲ 11.6 "
□ 13.1 "
Re ρ_{31}
Re ρ_{3-1}
0.4
0.2
0
-0.2
0.1
0.3
0.5
0.6
- t (GeV/c)^2

Fig. 12

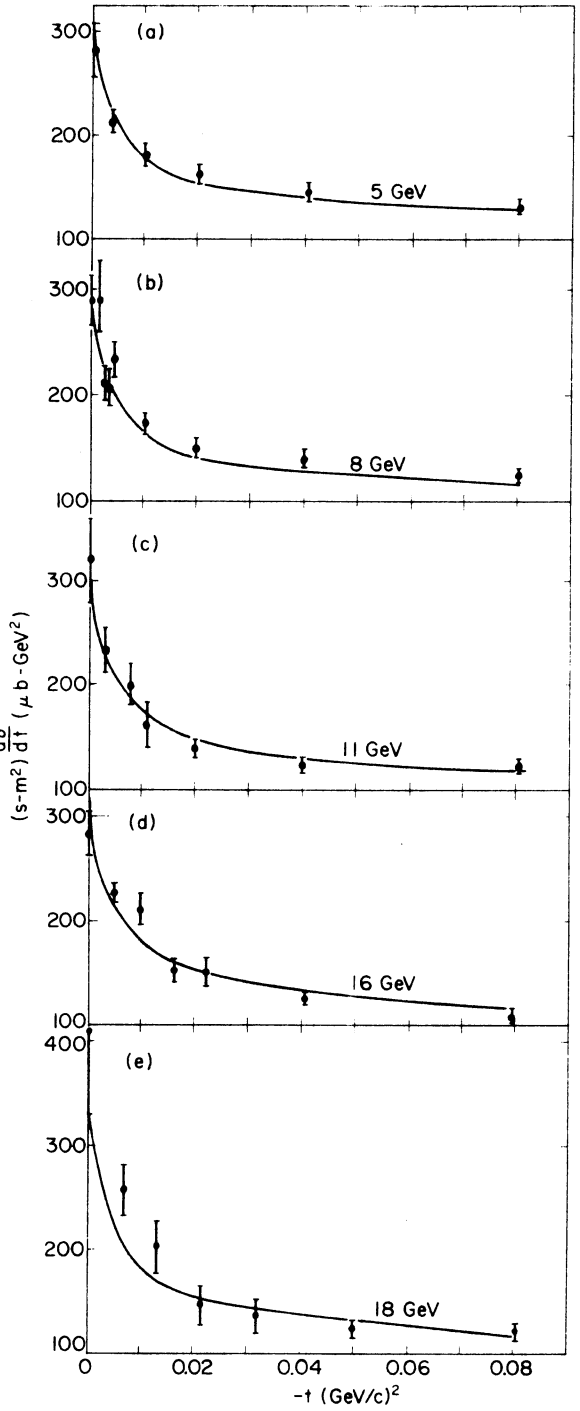
(a)
5 GeV
(b)
8 GeV
(c)
11 GeV
(d)
16 GeV
(e)
18 GeV
300
200
100
400
0
0.02
0.04
0.06
0.08
$-t$ (GeV/c)^2
$\frac{d\sigma}{dt}$ (μb-GeV^2)
$(s-m^2)^2$

Fig. 13

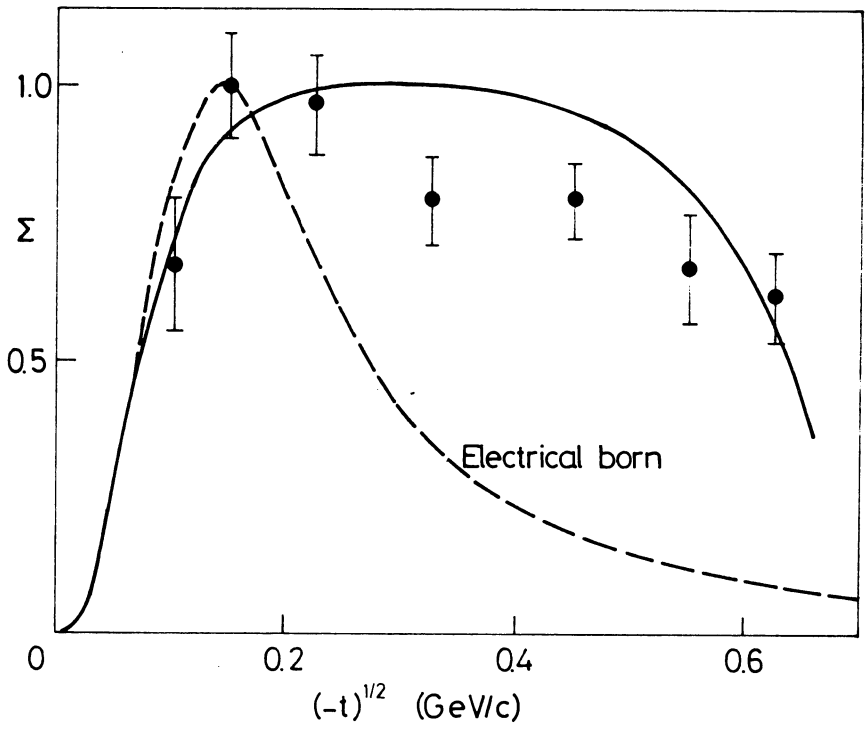

Fig. 14

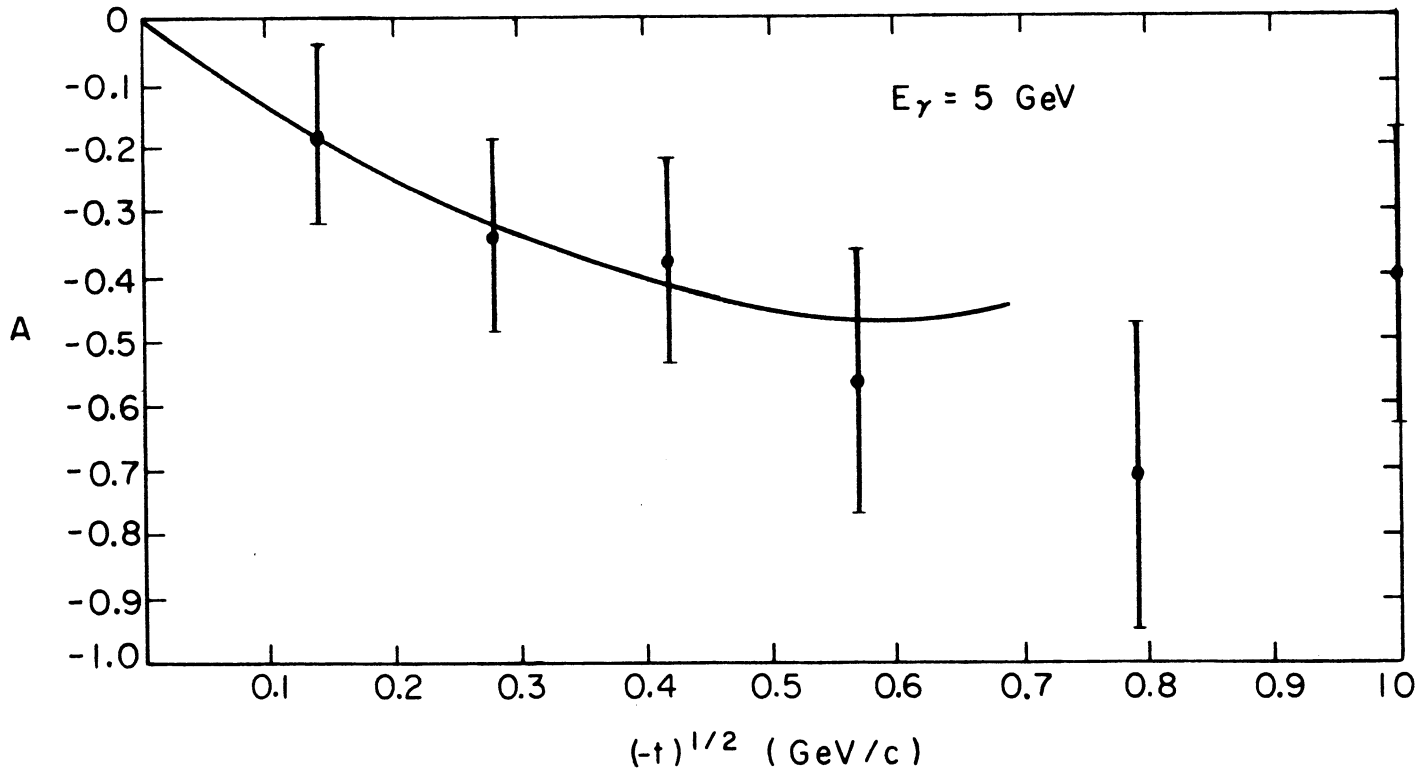
0
-0.1
-0.2
-0.3
-0.4
-0.5
-0.6
-0.7
-0.8
-0.9
-1.0
A
E_γ = 5 GeV
0.1
0.2
0.3
0.4
0.5
0.6
0.7
0.8
0.9
10
$(-t)^{1/2}$ (GeV/c)

Fig. 15